processes

MDPI

Article

3D Printer Nozzle Structure Form Optimal Structural Analysis

Yun Yu †, Gen Zhang †, Qiming Xiao *, Anping Ji, Yueqiang Feng, Guangyao Zhu and Lang Zhou

School of Mechanical Engineering, Chongqing Three Gorges University, No. 666, Tianxing Road, Baianba Street, Wanzhou District, Chongqing 404188, China; yuyun0405@163.com (Y.Y.); zhanggen0607@163.com (G.Z.); japmail721@163.com (A.J.); fengyq1232024@163.com (Y.F.); gegou5338@163.com (G.Z.); zl777998@163.com (L.Z.)

* Correspondence: xqmhust@163.com

† These authors should be considered joint first authors.

Abstract: The most representative technology of 3D printing is fused deposition modeling (FDM). To improve the printing accuracy of FDM technology, this paper first takes the outlet diameter, angle of convergence, and rectifier section length of the nozzle as the influencing factors. It takes the melt outlet speed stability, viscosity, and outlet pressure as the indexes to design the orthogonal test. Then, COMSOL Multiphysics fluid–solid coupling simulation was used to simulate and analyze the structural characteristics of the 3D printer nozzle, and the range analysis method was used to analyze the data. Finally, the two-phase flow combination was used to simulate the morphological characteristics of the melt flowing out of the nozzle. The results show that the simulation results of the two materials are similar. As the nozzle diameter decreases, the melt pressure decreases, the velocity increases, and the viscosity decreases. For PLA wire rods, the optimal structure of the nozzle is that the outlet diameter is 0.2 mm, the rectifier section length is 1.5 mm, and the angle of convergence is 60°. For ABS wire, the optimum structure of the nozzle is that the outlet diameter is 0.2 mm, the rectifier section length is 1.5 mm, and the angle of convergence is 30°. The nozzle outlet diameter is inversely proportional to the printing accuracy for ABS and PLA materials. The research results provide a theoretical reference for optimizing the nozzle structure for 3D printing.

Keywords: 3D printing; FDM technology; COMSOL simulation; nozzle structure; orthogonal test

Citation: Yu, Y.; Zhang, G.; Xiao, Q.; Ji, A.; Feng, Y.; Zhu, G.; Zhou, L. 3D Printer Nozzle Structure Form Optimal Structural Analysis. *Processes* **2024**, *12*, 1482. https://doi.org/10.3390/pr12071482

Academic Editor: Juan García Rodríguez

Received: 5 June 2024
Revised: 6 July 2024
Accepted: 8 July 2024
Published: 15 July 2024

1. Research Content and Significance of This Paper

Three-dimensional (3D) printing, also known as additive manufacturing, is an advanced manufacturing technology widely used at present. It is characterized by personalized processing based on digital models, simplifying the process of design and manufacturing, and reducing the threshold of manufacturing [1,2]. Fused deposition modeling (FDM) is one of the most representative, which mainly uses high temperature to melt the material into liquid, then solidifies it after extrusion by the print head, and finally arranges it in the three-dimensional space to form a three-dimensional object [3–5]. The technology mainly uses thermoplastic materials such as polylactic acid (PLA) and polyacrylonitrile–butadiene–styrene (ABS) as printing materials [6], which have the advantages of environmental protection, strong heat resistance, and good plasticity.

In the printing process, FDM technology is easily affected by factors such as the printing speed, nozzle, layer thickness, and printing platform temperature. The nozzle and layer thickness are the main factors affecting the parameters of the parts. The outlet speed stability, viscosity, and outlet pressure of the nozzle are important indicators reflecting the accuracy of 3D printing [7,8]. Parham et al. [9] explored the effect of printing speed on the tensile and fracture behavior of fused deposition molding ABS samples. The results showed that when the printing speed was 70 mm/s, it had the maximum elongation and fracture resistance, showing the best performance. Kieran et al. [10] found that increasing the layer thickness would reduce the mechanical properties of additive manufacturing polymer (PLA) and acrylonitrile–butadiene–styrene terpolymer (ABS). Yang et al. [11]

studied the effects of filling angle, printing speed, printing temperature, filling density, and layer thickness on the tensile strength of polylactic acid (PLA) specimens by combining single-factor and orthogonal test analysis. However, there is still a lack of optimization research on the nozzle structure of 3D printers. Most of the research focuses on condition monitoring or nozzle blockage monitoring, and many users rely on their own experience to qualitatively select the nozzle, which makes it challenging to select the most suitable nozzle structure [12,13].

Based on this, this paper uses COMSOL Multiphysics 6.0 to establish a two-dimensional axisymmetric model of the nozzle. The outlet diameter, angle of convergence, and rectifier section length are selected as the influencing factors, and the orthogonal test is carried out with the melt outlet speed stability, viscosity, and outlet pressure as the indexes. The models of different printing consumables (PLA, ABS) and different size structures are established. The fluid–solid coupling simulation analysis is used to simulate the velocity, pressure, and viscosity field of the filament in the nozzle by combining the orthogonal test. Through the range analysis of the data, the influence of the structural parameters of the nozzle on the indexes is judged, and the optimal nozzle structure is obtained by combining the morphology of the melt flowing out from the nozzle.

2. Experimental Design of Printed Materials

Orthogonal Experimental Design

According to the structural characteristics of the nozzle (as shown in Figure 1), the outlet speed stability, viscosity, and outlet pressure of the melt are mainly affected by the outlet diameter d1, the angle of convergence a, and the rectifier section length L [14]. It is found that high precision parts can be obtained when the nozzle outlet diameter of the 3D printer is 0.1–2.0 mm, the angle of convergence is 30°–60° and the rectifier section length is less than 2 mm [15,16]. Therefore, the three factors of outlet diameter, angle of convergence, and rectifier section length are selected in this paper, and three levels are set for the equidistant floating of each factor. The specific values are shown in Table 1. According to the principle of orthogonal test design, a three-factor and three-level orthogonal test table L_9 (3^3) was selected to carry out a total of nine groups of fluid–solid coupling simulation tests. The structural parameters of each group of nozzles are shown in Table 2.

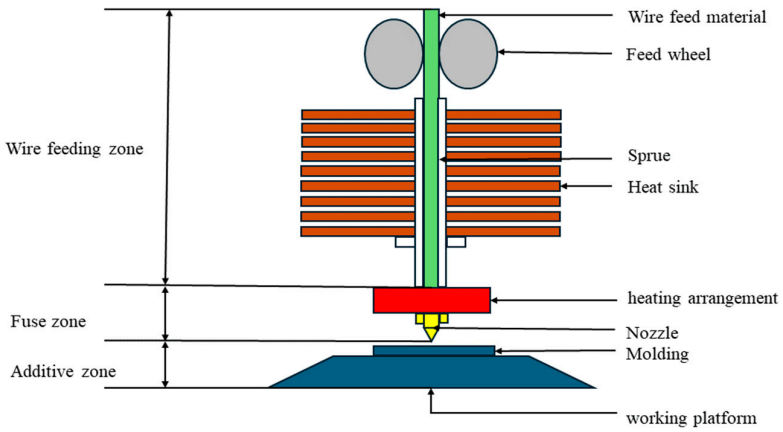

Figure 1. FDM nozzle working principle diagram.

Table 1. Orthogonal test factor levels.

Level	Outlet Diameter d1/mm	Angle of Convergence a/°	Rectifier Section Length L/mm
1	0.2	30	0.5
2	0.4	45	1
3	0.6	60	1.5

Table 2. Orthogonal test protocol table.

Test	Outlet Diameter d1/mm	Angle of Convergence a/°	Rectifier Section Length L/mm
1	0.2	30	0.5
2	0.2	45	1
3	0.2	60	1.5
4	0.4	60	0.5
5	0.4	45	1
6	0.4	30	1.5
7	0.6	45	0.5
8	0.6	60	1
9	0.6	30	1.5

3. Fluid–Solid Coupling Simulation Analysis

3.1. Simulation Model

The three-dimensional nozzle is cylindrical, allowing for consistency in geometry, loads, and constraints along its circumference. To simplify the analysis in COMSOL Multiphysics 6.0, a two-dimensional axisymmetric model of the nozzle is constructed using an orthogonal experimental program. This model enables coupled fluid–solid multiphysics field simulation, as depicted in Figure 2. Two-dimensional (2D) axisymmetric modeling offers a streamlined approach compared to 3D modeling, making it more efficient for model debugging and simpler for setting boundary conditions and mesh division.

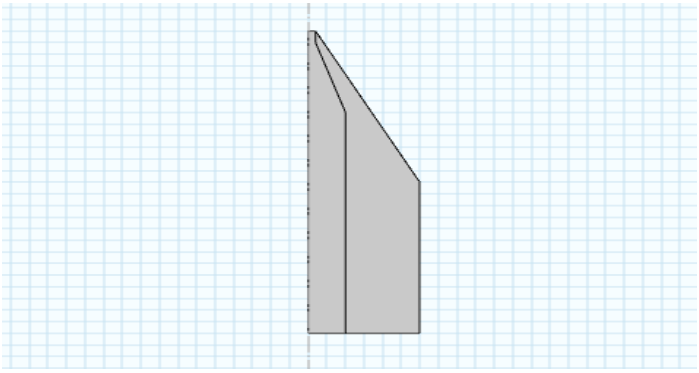

Figure 2. Two-dimensional axisymmetric simplified model of nozzle.

3.2. Material Properties

The fluid domain materials selected for the model simulation are PLA and ABS. The material parameters are shown in Table 3. The material used for the nozzle model in 3D printers is brass. Brass is chosen due to its good thermal conductivity and wear resistance, which are essential for material ejection and molding during the 3D printing process. Brass nozzles are capable of withstanding high-temperature and pressure environments while maintaining a stable nozzle diameter and aperture. This stability is beneficial for producing high-quality printed products. The brass parameters are detailed in Table 4 [17].

Table 3. Melt PLA and ABS material parameter table.

	Thermal Conductivity W/m·°C	Density kg/m^3	Coefficient of Thermal Expansion K^{-1}	Poisson's Ratio	Temperature T/deg
PLA	0.231	1200	1.999×10^{-6}	0.36	220
ABS	0.032	1150	8.38×10^{-5}	0.41	240

Table 4. Brass material parameter table.

Thermal Conductivity W/m·°C	Density kg/m^3	Coefficient of Thermal Expansion K^{-1}	Poisson's Ratio	Specific Heat Capacity J·kg^{-1}·K^{-1}
130	8500	1.65×10^{-5}	0.3	0.38

3.2.1. Simulation Settings

The 3D printing consumables ABS and PLA are high-molecular polymers. When they are heated to the molten state by FDM technology, their physical properties will be modified. At this time, the two materials can be approximated as Newton liquid [18,19]. When COMSOL is used to analyze the fluid–solid coupling multiphysical field, the fluid Reynolds number can be calculated to determine whether the fluid is laminar or turbulent. The calculation formula is shown in (1).

$$Re = \frac{\rho v d}{u} \tag{1}$$

where v is the flow velocity of the melt at the nozzle inlet, unit mm/s; d is the diameter of the nozzle inlet, unit mm; u is the melt dynamic viscosity, unit Pa-s; and ρ is the density of the melt, unit kg/m^3:

The Reynolds number of the two materials is calculated to be much less than 2300, indicating that the flow field in the nozzle is laminar. Therefore, in the simulation setting, the flow characteristics are set to laminar flow.

3.2.2. Boundary Condition Setting

According to the working principle of ABS and PLA melt extrusion 3D printing and the characteristics of the two-dimensional simulation model of the local flow channel, to obtain higher accuracy of the workpiece model, the printing layer height is selected to be 0.1 mm, the feed speed of the feed wheel is 0.5 mm/s, and the nozzle inlet diameter is 2 mm. By introducing the relevant parameters into the formula (2), the outlet flow rate of the nozzle can be calculated to be 1.57 mm^3/s.

$$v = \frac{v_s \pi d^2}{4} \tag{2}$$

where ν is the inlet flow rate in mm^3/s; ν_s is the wire feed rate in mm/s; and d is the inlet diameter.

We set the laminar flow inlet boundary condition as a fully developed flow with a flow rate of 1.57 mm^3/s.

3.2.3. Image Analysis of Simulation Results

In the nine groups of simulation results of PLA and ABS, the distribution of velocity, pressure, and viscosity field is similar. Therefore, PLA test 9 is used as an example. The distribution of nozzle melt pressure field at the exit surface, as shown in Figure 3, reveals that the melt pressure decreases along the axis toward the exit due to the nozzle's pressure drop type structure. The most significant change in pressure drop occurs within the rectification section and the conical shrinkage area. This indicates that the change in the diameter of the cross-section will lead to the increase in the internal resistance and pressure drop of the melt; at the same time, the melt pressure on the outlet surface remains relatively small and stable. At this time, the molten material can be smoothly extruded and stacked.

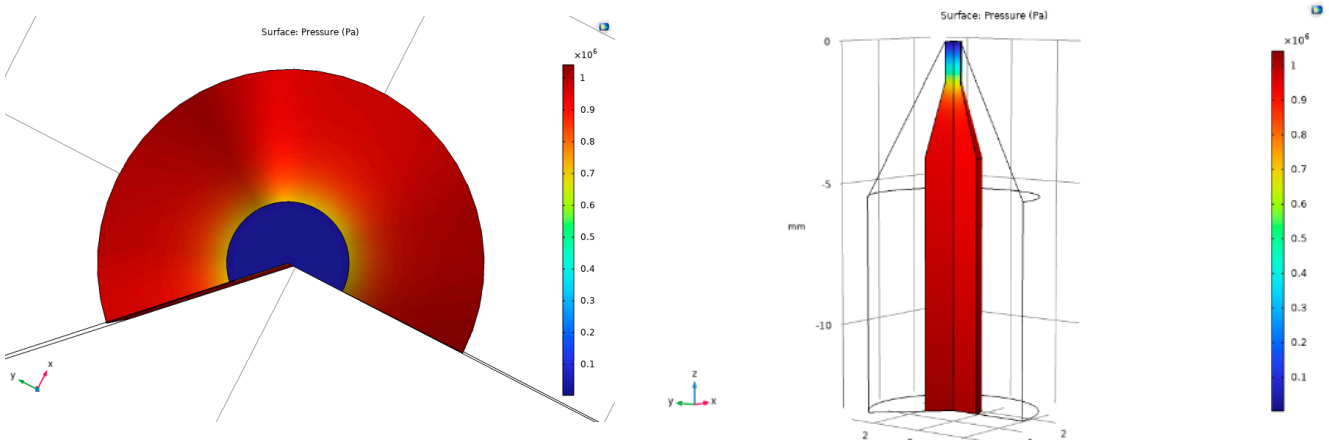

Figure 3. Melt pressure field distribution.

The steady-state analysis of the nozzle velocity field distribution is presented in Figure 4. From the analysis, it can be concluded that the velocity change in the melt entering the flow channel is minimal. However, there is an increase in velocity as the nozzle diameter shrinks. In the rectification section, the overall melt velocity is higher: the maximum speed at the outlet surface. This phenomenon occurs because the incompressible fluid flows from a large-diameter pipe to a small-diameter pipe, requiring an increase in flow rate to maintain fluid volume conservation. As a result, there is a significant increase in velocity as the melt flows through the narrow flow channel. At the nozzle exit surface, the velocity is highest in the middle and gradually decreases toward the edges. This distribution pattern is attributed to the high viscosity of the melt, causing the velocity near the wall to be close to zero and gradually increasing toward the center of the flow channel.

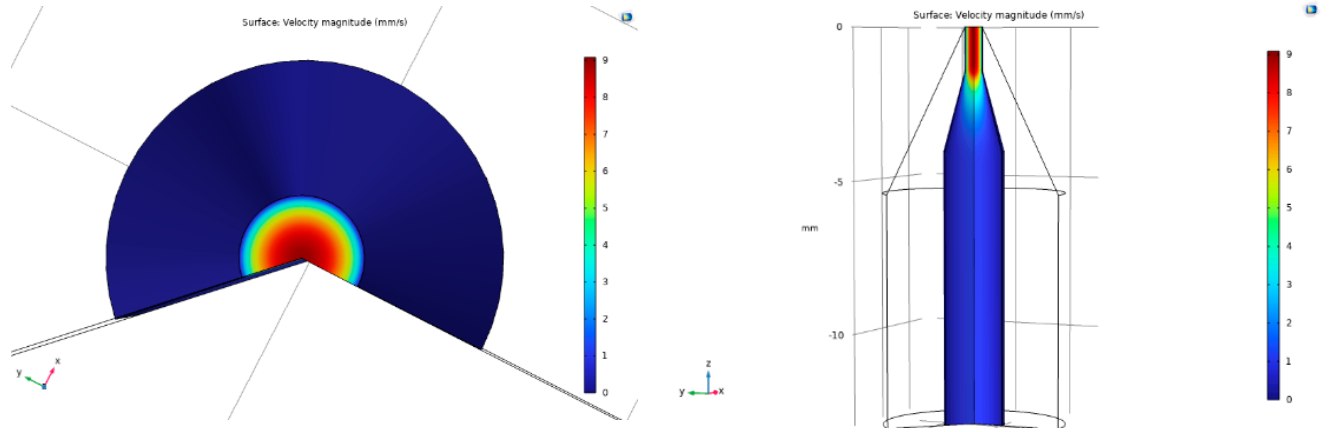

Figure 4. Melt velocity field distribution.

The distribution of melt viscosity in the nozzle is illustrated in Figure 5. As the diameter of the flow channel decreases, the shear rate in the flow channel increases. This leads to a gradual decrease in the viscosity of the polymer melt, exhibiting shear thinning characteristics. Additionally, the viscosity is smaller closer to the wall [20].

Through the analysis of the simulation results of the pressure field distribution, velocity field distribution, and viscosity field distribution of the melt, it can be found that the pressure, velocity, and viscosity of the melt are affected by the outlet diameter, angle of convergence, and rectifier section length of the nozzle.

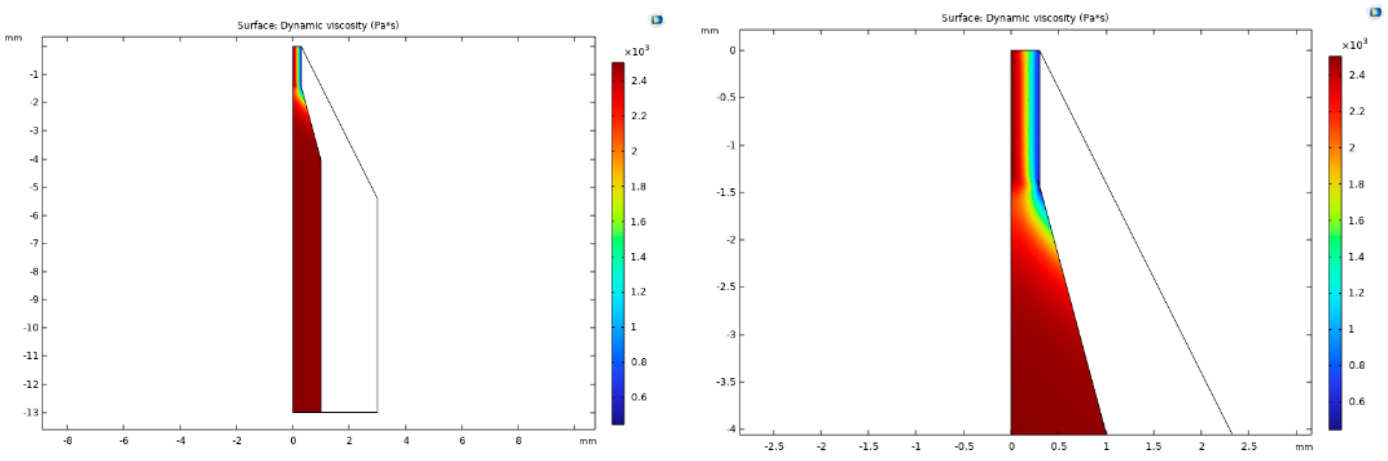

Figure 5. Melt viscosity field distribution in the nozzle.

3.2.4. Flow Orthogonal Test with Different-Sized Nozzles

According to the model established by nine groups of orthogonal experiments of each material, the simulation data are shown in Tables 5 and 6. In the post-processing of the results, the outlet velocity distribution, the outlet surface pressure value, and the average viscosity of the center of the rectifier section are the research objects.

Table 5. Simulation results of orthogonal test—PLA.

Trial	Outlet Diameter d1/mm	Angle of Convergence a/°	Rectifier Section Length L/mm	Variance of Exit Speed /mm^2·s^{-2}	Outlet Pressure /Pa	Melt Viscosity /Pa·s
1	0.2	30	0.5	584.85	25,483	690.5489
2	0.2	45	1	568.6116	27,336	1922.853
3	0.2	60	1.5	481.4977	72,701	817.7251
4	0.4	60	0.5	43.22925	10,368	2395.872
5	0.4	45	1	43.21376	10,858	2438.399
6	0.4	30	1.5	38.80241	13,207	2356.689
7	0.6	45	0.5	10.23675	6356.6	2430.951
8	0.6	60	1	9.87244	8767.1	2444.052
9	0.6	30	1.5	9.910075	6904.9	2447.821

Table 6. Orthogonal test simulation results—ABS.

Trial	Outlet Diameter d1/mm	Angle of Convergence a/°	Rectifier Section Length L/mm	The Variance of Exit Speed/mm^2·s^{-2}	Outlet Pressure /Pa	Melt Viscosity /Pa·s
1	0.2	30	0.5	721.0796	38,324	694.3866
2	0.2	45	1	904.8836	35,643	682.8386
3	0.2	60	1.5	800.0689	76,954	312.5136
4	0.4	60	0.5	63.18553	7485.4	1890.577
5	0.4	45	1	63.6836	7686.6	2040.533
6	0.4	30	1.5	56.60129	10,256	1272.485
7	0.6	45	0.5	12.49664	4096.5	2297.323
8	0.6	60	1	12.15003	5721.9	2398.528
9	0.6	30	1.5	12.22153	4565.4	2459.815

4. Simulation Data Analysis

4.1. Range Analysis

Range analysis is a statistical method used to evaluate the difference between the maximum and minimum values in a data set. It is commonly employed by researchers to assess the degree of variation and distribution within data sets as well as to compare variations between different groups [21]. This analysis technique finds application in diverse fields,

including market research, medical research, and ecological studies. The calculation process for range analysis is straightforward and easily comprehensible, enabling researchers to obtain optimization results through simple calculations and judgments. Furthermore, it allows the determination of the extent to which each factor influences the index. Range analysis formulas, such as Equations (3) and (4), can be used for this purpose.

$$\overline{K_{ij}} = \frac{K_{ij}}{s} \tag{3}$$

$$R_j = max\overline{K_{ij}} - min\overline{K_{ij}} \tag{4}$$

where $\overline{K_{ij}}$ is the average of all results of a test index when the j factor is taken at the i level; K_{ij} is the sum of all results of a test index when the j factor takes the i level; R_j is the range of the factors in column j.

4.2. PLA Filament Range Analysis Results

4.2.1. Analysis of Variance of Export Velocity

The polar analysis table of exit velocity variance is calculated using Equations (3) and (4), as shown in Table 7. From the table, it is evident that all three variables have a positive impact on the stability of the exit velocity. However, among the three variables (outlet diameter, rectifier section length, and angle of convergence), the outlet diameter has the greatest influence on the stability of the nozzle melt's exit speed. On the other hand, the rectifier section length and angle of convergence have a relatively smaller effect. Therefore, when the nozzle outlet diameter is 0.6 mm, the rectifier section length is 1.5 mm, and the angle of convergence is 60°, a more stable outlet velocity can be achieved.

Table 7. Export velocity variance range analysis table -PLA.

	A	B	C
Level	**Outlet Diameter**	**Rectifier Section Length**	**Angle of Convergence**
K1	1634.959	638.315997	633.56
K2	125.2454	621.697835	622.06
K3	30.01927	530.210138	534.6
K1 mean	544.9864	212.771999	211.19
K2 mean	41.74847	207.232612	207.35
K3 mean	10.00642	176.736713	178.2
Range R	534.98	36.0352861	32.988
Primary and secondary order	1	3	2
Excellent level	A3	B3	C3

4.2.2. Outlet Surface Pressure Analysis

Table 8 presents the analysis of the average pressure range on the surface of the nozzle outlet. It can be concluded that the outlet diameter has the greatest influence on the melt outlet pressure compared to the rectifier section length and angle of convergence of the rectifier section. Additionally, the range values of the rectifier section length and angle of convergence are also significant factors affecting the pressure. Based on the optimal combination determined through range analysis, it is recommended to use an outlet diameter of 0.1 mm, a rectifier section length of 1.5 mm, and an angle of convergence of 60° to achieve higher outlet pressure and ensure smooth melt extrusion.

Table 8. Outlet pressure range analysis table—PLA.

	A	B	C
Level	**Outlet Diameter**	**Rectifier Section Length**	**Angle of Convergence**
K1	125,520	42,207.6	45,594.9
K2	34,433	46,961.1	44,550.6
K3	22,028.6	92,812.9	91,836.1
K1 mean	41,840	14,069.2	15,198.3
K2 mean	11,477.66667	15,653.7	14,850.2
K3 mean	7342.866667	30,937.63333	30,612.03333
Range R	34,497.13333	16,868.43333	15,761.83333
Primary and secondary order	1	2	3
Excellent level	A1	B3	C3

4.2.3. Melt Viscosity Analysis in the Rectifier Section

The influence degree of the runner viscosity of the three factors was calculated by taking the mean value of the axial viscosity of the rectification section as the test index. Table 9 shows that compared with the rectifier section length and the angle of convergence, the outlet diameter has the greatest influence on the viscosity in the rectification section, while the rectifier section length and the angle of convergence have a lesser influence on the viscosity. Based on the optimal combination derived from the extreme variance analysis, it can be concluded that the melt viscosity inside the nozzle is smaller and the melt fluidity is better when the outlet diameter is 0.1 mm, the rectifier section length is 1 mm, and the angle of convergence is 45°.

Table 9. Flow channel melt viscosity range analysis table.

Level	Outlet Diameter	Rectifier Section Length	Angle of Convergence
K1	3431.127451	5517.371663	5495.058684
K2	7190.959674	6805.303897	6792.202858
K3	7322.823305	5622.234869	5657.648887
K1 mean	1143.70915	1839.123888	1831.686228
K2 mean	2396.986558	2268.434632	2264.067619
K3 mean	2440.941102	1874.07829	1885.882962
Range R	1297.231951	429.3107448	432.3813913
Primary and secondary order	1	3	2
Excellent level	A1	B3	C1

4.2.4. Optimal Structural Analysis

Based on the range analysis results, it can be concluded that the factors with the greatest influence on outlet speed stability, outlet pressure, and runner viscosity are the outlet diameter, rectifier section length, and angle of convergence, in that order. The three optimal structural parameters were found to be A3B3C3, A1B3C3, and A1B1C1, corresponding to the stable outlet velocity, higher outlet pressure, and low runner viscosity, respectively. Using these three sets of structures, a nozzle model was established, and fluid–structure interaction simulation was conducted using COMSOL Multiphysics 6.0. The results, shown in Table 10, indicate that when the outlet diameter is 0.6 mm, the variance of the outlet velocity is only 1.72, resulting in a stable flow rate. However, the outlet pressure is low, which may hinder the smooth extrusion of the melt. On the other hand, when the outlet diameter is 0.2 mm, the outlet speed is relatively stable, the pressure is high, and the melt viscosity is low, allowing for high-precision and stable printing. Therefore, the optimal structure for printing PLA filament is an outlet diameter of 0.2 mm, a rectifier section length of 1.5 mm, and an angle of convergence of 60°.

Table 10. Comparison of three simulation results of PLA filament.

Serial Number	Outlet Diameter/mm	Rectifier Section Length/mm	Angle of Convergence/°	Export Speed Variance/mm^2·s^{-2}	Outlet Face Pressure/Pa	Runner Viscosity/Pa·s
1	0.6	1.5	60	1.724175301	3734.5	2480.96
2	0.2	1.5	60	77.91752212	24942	2007.73
3	0.2	0.5	30	584.852	25483	690.549

4.3. ABS Filament Range Analysis Results

4.3.1. Analysis of Variance of Export Velocity

Table 11 demonstrates that the outlet diameter has the most significant impact on the variance of the outlet velocity when the molten material is ABS. It is followed by the rectifier section length and angle of convergence of the rectifier section. The change in angle of convergence and the rectifier section length have a minimal effect on the outlet velocity. Notably, when the outlet diameter is 0.6 mm, the nozzle exit speed is observed to be smoother.

Table 11. Egress velocity ANOVA results.

	A	B	C
Level	**Outlet Diameter**	**Rectifier Section Length**	**Angle of Convergence**
K1	2426.032	796.7618	789.9024
K2	183.4704	980.7172	981.0638
K3	36.8682	868.8917	875.4044
K1 means	808.6773	265.5873	263.3008
K2 means	61.15681	326.9057	327.0213
K3 means	12.2894	289.6306	291.8015
Range R	796.3879	61.31849	63.72048
Primary and secondary order	1	3	2
Excellent level	A3	B1	C1

4.3.2. Outlet Surface Pressure Analysis

The range analysis of the nozzle outlet pressure is presented in Table 12. It can be concluded that the outlet pressure is significantly influenced by three factors, namely the outlet diameter, angle of convergence, and rectifier section length. Among these factors, the outlet diameter has the largest influence, which is followed by the angle of convergence and rectifier section length. As the outlet diameter increases, the pressure decreases, indicating that a larger diameter is not favorable for melt extrusion in the nozzle. On the other hand, the pressure increases with the increase in the other two factors. Therefore, for an outlet diameter of 0.2 mm, an angle of convergence of 60°, and a rectifier section length of 1.5 mm, a higher outlet pressure can be achieved to ensure smooth melt extrusion.

Table 12. Outlet face pressure range analysis.

	A	B	C
Level	**Outlet Diameter**	**Rectifier Section Length**	**Angle of Convergence**
K1	150,921	49,905.9	53,145.4
K2	25,428	49,051.5	47,426.1
K3	14,383.8	91,775.4	90,161.3
K1 mean	50,307	16,635.3	17,715.13
K2 mean	8476	16,350.5	15,808.7
K3 mean	4794.6	30,591.8	30,053.77
Range R	45,512.4	14,241.3	14,245.07
Primary and secondary order	1	3	2
Excellent level	A1	B3	C3

4.3.3. Melt Viscosity Analysis in the Rectifier Section

The results of the analysis on the range of melt viscosity for the rectifier can be found in Table 13. It is evident that among all the factors, the outlet diameter has the most significant impact on viscosity. As the outlet diameter increases, the shear strength of the nozzle wall decreases, leading to an increase in melt viscosity. On the other hand, the rectifier section length has a minimal effect on viscosity, as there is little change in the melt viscosity when the length is altered.

Table 13. Extreme analysis of melt viscosity in the rectifier section.

	A	**B**	**C**
Level	**Outlet Diameter**	**Rectifier Section Length**	**Angle of Convergence**
K1	1689.739	4882.287	4426.686
K2	5203.595	5121.9	5020.695
K3	7155.666	4044.813	4601.618
K1 means	563.2463	1627.429	1475.562
K2 means	1734.532	1707.3	1673.565
K3 means	2385.222	1348.271	1533.873
Range R	1821.976	359.0289	198.0031
Primary and secondary order	1	2	3
Excellent level	A1	B3	C1

4.3.4. Optimal Structural Analysis

Based on the extreme difference analysis results, it can be concluded that the outlet diameter has the greatest influence on three indicators and also has the greatest impact on ABS printing accuracy. When the outlet diameter of a 0.6 mm nozzle is used, the exit speed is more stable. On the other hand, a 0.2 mm nozzle results in higher exit pressure and lower melt viscosity, leading to better fluidity. The optimal combination of these indicators was simulated and analyzed, and the results are presented in Table 14. Considering the printing accuracy of the parts, the best outcome is achieved when using a nozzle outlet diameter of 0.2 mm, a rectifier section length of 1.5 mm, and an angle of convergence of 30° for ABS wire printing.

Table 14. Comparison of three simulation results of ABS filament.

Serial Number	**Outlet Diameter/mm**	**Rectifier Section Length/mm**	**Angle of Convergence/°**	**Export Speed Variance/mm^2·s^{-2}**	**Outlet Face Pressure/Pa**	**Runner Viscosity/Pa·s**
1	0.6	0.5	30	1.21470364	7676.2	31710.1
2	0.2	1.5	60	800.0688631	76954	312.5136
3	0.2	1.5	30	91.04141617	34524	356.629

5. Nozzle Extrusion Melt Morphology Analysis

5.1. Analysis Objects

This chapter focuses on analyzing the combination of three sets of optimal horizontal structure parameters obtained through the range analysis of two materials. The objective is to examine the average radius of multiple positions of the liquid column when it flows out of the nozzle during the printing process of an FDM fused deposition 3D printer. A smaller difference between the average radius and the nozzle outlet radius indicates that the nozzle with this structure is better suited to meet the printing requirements. The specific test settings are shown in Table 15.

Table 15. Morphology analysis experimental group.

	Serial Number	Outlet Diameter/mm	Rectifier Section Length/mm	Angle of Convergence/°
PLA	1	0.6	1.5	60
	2	0.2	1.5	60
	3	0.2	0.5	30
ABS	1	0.6	0.5	30
	2	0.2	1.5	60
	3	0.2	1.5	30

5.2. Simulation Settings

To investigate the morphological characteristics of the liquid column formed when the melt flows out of the nozzle, the flow of melt from the nozzle into the air needs to be simulated using the COMSOL Multiphysics 6.0 software. When selecting the physics simulation interface, the 'Laminar Two-Phase Flow, Phase Field' Multiphysics interface should be chosen, as it allows for tracking the interface between two immiscible fluids.

The simulation model, as depicted in Figure 6, consists of an upper rectangular section representing the air domain and a lower section representing the internal flow channel of the nozzle. The melt enters the nozzle from the lower nozzle inlet at a flow rate of 0.57 mm^3/s, and it is a fully developed flow.

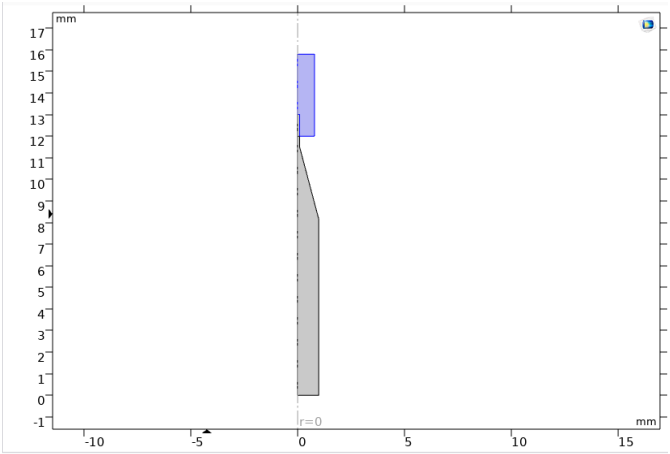

Figure 6. Nozzle two-phase flow simulation model.

5.3. Analysis of Simulation Results

5.3.1. Microextrusion Release Mold Expansion Effect

The FDM-type fused deposition process utilizes microextrusion technology. The plastic melt in this process has a long-chain molecular structure. As the plastic melt passes through the nozzle flow channel, the diameter of the flow channel changes abruptly due to the pressure drop. This causes the molecular long-chain structure of the plastic melt to stretch, resulting in an end effect. The end effect is a result of the elastic behavior of the polymer melt during processing. When the polymer flows out of the tube, it undergoes strong stretching and elastic deformation while flowing through the nozzle. However, these deformations are only partially recovered in the nozzle, leading to lateral expansion of the melt when it exits the outlet. This expansion of the melt has been observed [22–24].

For FDM printing consumables, when the material is heated and melted, it becomes a molten state. As the melt flows out of the nozzle, the diameter of the melt is not the same as the nozzle outlet diameter. The diameter of the melt liquid column expands more than the diameter of the nozzle. This expansion phenomenon is known as extrusion expansion. Figure 7a–f illustrates the occurrence of extrusion expansion in molten PLA and ABS

extrusion nozzles, indicating that the COMSOL simulation model accurately represents the outflow of FDM fused deposition 3D printing melt.

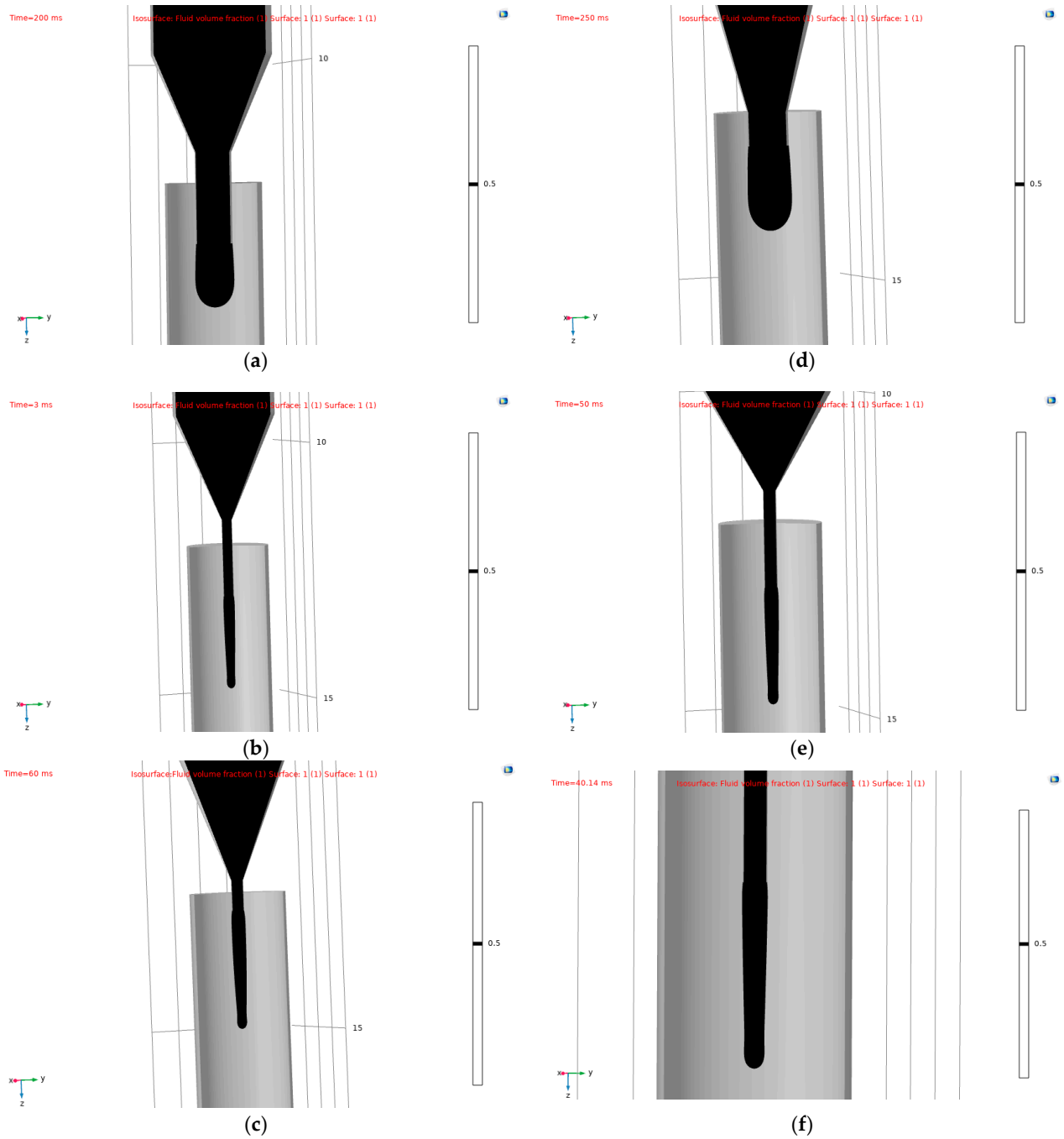

Figure 7. (**a**–**f**) Melt extrusion expansion phenomenon.

5.3.2. Comparison of Melt Morphology

Based on the results shown in Figure 8 of the PLA test simulation, it is evident that the diameter of the nozzle outlet significantly affects the shape of the melt outflow, particularly the morphology of the liquid column. Specifically, when the outlet diameter is 0.6 mm, the liquid column appears to be shorter and thicker. On the other hand, when the outlet diameter is reduced to 0.2 mm, the liquid column becomes slender, thereby enabling higher precision printing.

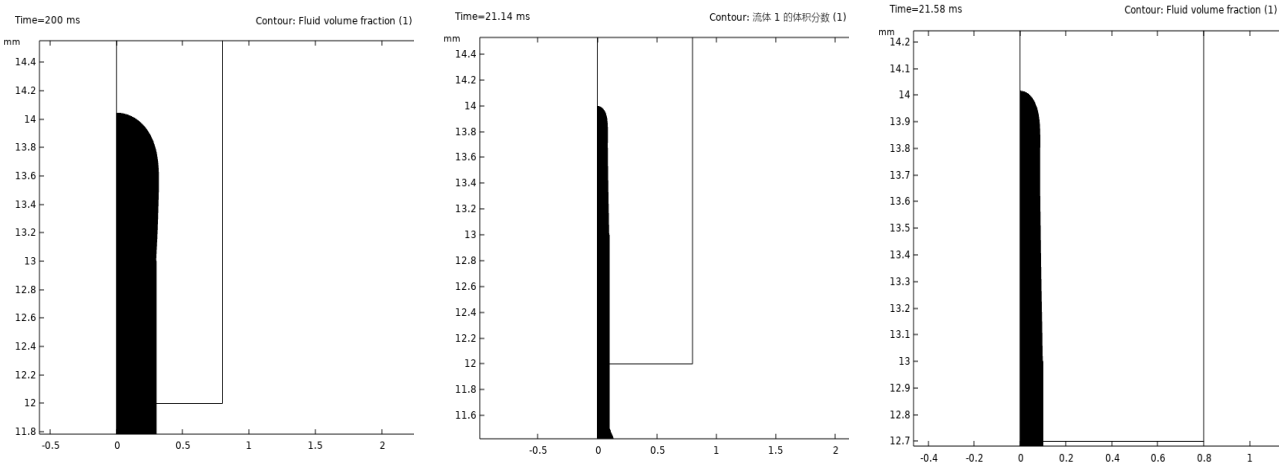

Figure 8. Morphology when the PLA melt flows out of a 1 mm nozzle.

By integrating the line in the COMSOL result processing, the radius value at different heights of the outflow 1 mm liquid column is calculated and compared with the nozzle outlet diameter. The calculation results are shown in Table 16. It can be concluded that for the three nozzle structures, there is a certain deviation between the melt radius of the outflow and the nozzle outlet diameter. The smallest deviation, approximately 0.006 mm, is observed when the nozzle outlet diameter is 0.2 mm, the rectifier section length is 0.5, and the angle of convergence is 30°.

Table 16. PLA liquid column radius comparison.

Experiment	Position 1	Position 2	Position 3	Position 4	Mean	Difference
1	0.31304	0.32045	0.32426	0.29826	0.314003	0.014003
2	0.11436	0.11388	0.11179	0.10816	0.112048	0.012048
3	0.096899	0.094507	0.092319	0.093152	0.094219	0.005781

According to the results of the ABS test simulation Figure 9, the morphology and morphological characteristics of the melt when it flows out of a 1 mm nozzle are similar to that of PLA melt. The radius values obtained from the three sets of tests are presented in Table 17. It can be inferred that the smallest deviation, approximately 0.006 mm, occurs when the nozzle outlet diameter is 0.2 mm, the rectifier section length is 1.5, and the angle of convergence is 60°.

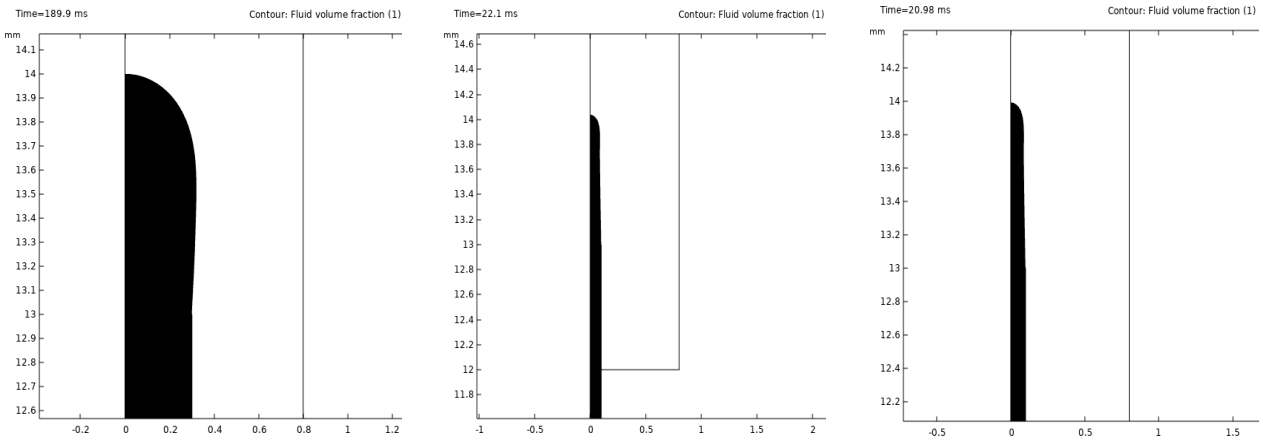

Figure 9. Morphology when ABS melt flows out of 1 mm.

Table 17. ABS column radius comparison.

Experiment	Position 1	Position 2	Position 3	Position 4	Mean	Difference
1	0.31284	0.288	0.076304	0.003927	0.170268	0.129732
2	0.097157	0.094631	0.092266	0.093396	0.094363	0.005637
3	0.097308	0.094767	0.092358	0.092775	0.094302	0.005698

6. Summary

This paper aims to analyze the influence of nozzle outlet diameter, angle of convergence, and rectifier section length on the flow field in the nozzle of a 3D printer. The analysis is carried out using COMSOL Multiphysics fluid–solid coupling multiphysics simulation. The advantage of this method is that the influence of other related variables can be controlled, and only the nozzle outlet diameter, angle of convergence, and rectifier section length are studied. The study also examines the influence of these factors on the stability of the outlet velocity, runner viscosity, and outlet pressure using the range analysis method. Additionally, the paper simulates the morphological characteristics of melt outflow nozzles combined with two-phase flow and analyzes the optimal nozzle structure suitable for PLA and ABS printing wire. Based on the analysis, the following conclusions were drawn:

(1) For a PLA wire rod, when considering the stability of the outlet velocity: nozzle outlet diameter > angle of convergence > rectifier section length; when considering the influence of the outlet pressure: nozzle outlet diameter > rectifier section length > angle of convergence; when considering the influence of the viscosity of the flow channel: outlet diameter > angle of convergence > rectifier section length. Through the extreme difference analysis of the simulation data, the optimal structure of the PLA wire printing nozzle is determined to be an outlet diameter of 0.2 mm, a rectifier section length of 1.5 mm, and an angle of convergence of 60°.

(2) For ABS wire, when considering the stability of the outlet speed: nozzle outlet diameter > angle of convergence > rectifier section length; when considering the outlet pressure: nozzle outlet diameter > angle of convergence > rectifier section length; when considering the viscosity stability of the flow channel: outlet diameter > angle of convergence > rectifier section length. Through simulation analysis, the optimal structure of the printing ABS wire nozzle is determined to be an outlet diameter of 0.2 mm, a rectifier section length of 1.5 mm, and an angle of convergence of 30°.

(3) The extrusion process of ABS and PLA melt in a 3D printing nozzle was simulated by COMSOL two-phase flow simulation. We observed the extrusion expansion effect of the melt as it flowed out of the nozzle and measured the radius of the liquid column at different heights when the melt flowed out of a 1 mm opening. We compared the nozzle outlet diameter with the radius of the liquid column and found that when the outlet diameter is smaller, the radius of the liquid column is closer to the nozzle outlet diameter. This shows that ABS and PLA are two materials for which using a smaller outlet diameter can achieve higher accuracy.

Author Contributions: Conceptualization, Y.Y., G.Z. (Gen Zhang) and A.J.; Methodology, Y.Y., G.Z. (Gen Zhang) and Q.X.; Software, Y.Y.; Validation, Y.Y. and A.J.; Formal analysis, Y.Y. and G.Z. (Gen Zhang); Investigation, Y.Y. and Y.F.; Resources, Q.X., G.Z. (Guangyao Zhu) and L.Z.; Data curation, Q.X.; Writing—original draft, Y.Y.; Writing—review & editing, G.Z. (Gen Zhang). All authors have read and agreed to the published version of the manuscript.

Funding: This research received no external funding.

Data Availability Statement: The original contributions presented in the study are included in the article, further inquiries can be directed to the corresponding author.

Conflicts of Interest: The authors declare no conflict of interest.

References

1. MacDonald, E.; Wicker, R. Multiprocess 3D printing for increasing component functionality. *Science* **2016**, *353*, aaf2093. [CrossRef] [PubMed]
2. Ng, W.L.; An, J.; Chua, C.K. Process, material, and regulatory considerations for 3D printed medical devices and tissue constructs. *Engineering* **2024**. [CrossRef]
3. Peng, M.; Liu, S.; Wei, Z.; Feng, X.; Lu, M.; Li, D.; Xu, J. Orthogonal experimental study on BST/PVDF-ABS composites fabricated with FDM additive materials. *J. Compos.* **2024**, 1–10.
4. Sun, J.; Zhou, W.; Huang, D.; Fuh, J.Y.H.; Hong, G.S. An overview of 3D printing technologies for food fabrication. *Food Bioprocess Technol.* **2015**, *8*, 1605–1615. [CrossRef]
5. Ren, L. Design and Simulation of FDM Screw Extrusion 3D Printer. Master's Thesis, Shaanxi University of Technology, Hanzhong, China, 2022.
6. Zhu, Y.; Du, M.; Lu, C.; Yin, J.; Zheng, Q. Effect of 3D printing TPU soft material process parameters on interlayer adhesion. *Chin. J. Polym.* **2018**, *4*, 532–540.
7. Triyono, J.; Sukanto, H.; Saputra, R.M.; Smaradhana, D.F. The effect of nozzle hole diameter of 3D printing on porosity and tensile strength parts using polylactic acid material. *Open Eng.* **2020**, *10*, 762–768. [CrossRef]
8. Syrlybayev, D.; Zharylkassyn, B.; Seisekulova, A.; Akhmetov, M.; Perveen, A.; Talamona, D. Optimization of Strength Properties of FDM Printed Parts—A Critical Review. *Polymers* **2021**, *13*, 1587. [CrossRef] [PubMed]
9. Rezaeian, P.; Ayatollahi, M.R.; Nabavi-Kivi, A.; Razavi, N. Effect of printing speed on tensile and fracture behavior of ABS specimens produced by fused deposition modeling. *Eng. Fract. Mech.* **2022**, *266*, 108393. [CrossRef]
10. Shergill, K.; Chen, Y.; Bull, S. An investigation into the layer thickness effect on the mechanical properties of additively manufactured polymers: PLA and ABS. *Int. J. Adv. Manuf. Technol.* **2023**, *126*, 3651–3665. [CrossRef]
11. Yang, L.; Meng, J.; Xue, T. Effect of 3D printing process parameters on tensile strength of PLA specimens. *Plast. Ind.* **2021**, *49*, 73–77+142.
12. Tlegenov, Y.; Hong, G.S.; Lu, W.F. Nozzle condition monitoring in 3D printing. *Robot. Comput. Manuf.* **2018**, *54*, 45–55. [CrossRef]
13. Tlegenov, Y.; Wong, Y.S.; Hong, G.S. A dynamic model for nozzle clog monitoring in fused deposition modelling. *Rapid Prototyp. J.* **2017**, *23*, 391–400. [CrossRef]
14. Zhao, H.; Zhang, Y.; Zhang, Y. Nozzle optimization design of core 3D printing device. *China Pet. Mach.* **2017**, *45*, 11–15.
15. Ren, C.; Yan, K.; Fan, L. Study on Process Parameters of Fused Deposition Rapid Prototyping Nozzle Based on FLUENT Simulation. *Foundry Technol.* **2017**, *38*, 1406–1409.
16. Tang, G.; Xu, W.; Wu, Q.; Lu, Y. Optimized design of three-dimensional printing nozzle structure based on ANSYS CFX. *J. Guizhou Norm. Univ.* **2014**, *32*, 96–99.
17. Zhang, T.; Luo, X.; Guo, L.; Zhang, L.; Tang, X.; Li, J.; Cheng, J.; Li, Y.; Qin, Q. *Mechanics of Materials*; Chongqing University Press: Chongqing, China, 2018.
18. Fernández, J.; Etxeberria, A.; Sarasua, J. Synthesis, structure and properties of poly(L-lactide-co-ε-caprolactone) statistical copolymers. *J. Mech. Behav. Biomed. Mater.* **2012**, *9*, 100–112. [CrossRef] [PubMed]
19. Yu, K. Design and Process Research on Pneumatic Melt Extrusion 3D Printing Nozzle *D*. Harbin Institute of Technology: Harbin, China, 2022.
20. Coogan, T.J.; Kazmer, D.O. In-line rheological monitoring of fused deposition modeling. *J. Rheol.* **2019**, *63*, 141–155. [CrossRef]
21. Wu, X. Rheological Behavior Analysis of Micro Extrusion Melt and Research on Screw Optimization Design. Ph.D. Thesis, South China University of Technology, Guangzhou, China, 2010.
22. Luo, J.; Zeng, G.; Li, B. Simulation and analysis of two-phase flow field in nozzle hole based on FLUENT. *J. Modul. Mach. Tools Autom. Process. Technol.* **2016**, *10*, 44–47.
23. Heller, B.P.; Smith, D.E.; Jack, D.A. Effects of extrudate swell and nozzle geometry on fiber orientation infused filament fabrication nozzle flow. *J. Addit. Manuf.* **2016**, *12*, 252–264.
24. Samy, A.A.; Golbang, A.; Harkin-Jones, E.; Archer, E.; McIlhagger, A. Prediction of part distortion in Fused Deposition Modelling (FDM) of semi-crystalline polymers via COMSOL: Effect of printing conditions. *CIRP J. Manuf. Sci. Technol.* **2021**, *33*, 443–453. [CrossRef]